Cell Stem Cell
Article

A Specialized Vascular Niche for Adult Neural Stem Cells

Masoud Tavazoie,[1] Lieven Van der Veken,[1,5] Violeta Silva-Vargas,[2,5] Marjorie Louissaint,[2] Lucrezia Colonna,[2] Bushra Zaidi,[2] Jose Manuel Garcia-Verdugo,[4] and Fiona Doetsch[1,2,3,*]
[1]Department of Neuroscience
[2]Department of Pathology and Cell Biology
[3]Department of Neurology
College of Physicians and Surgeons, Columbia University, New York City, NY, 10032 USA
[4]Instituto Cavanilles, Centro de Investigación Principe Felipe, Universidad de Valencia, Burjassot-46100, Valencia, Spain
[5]These authors contributed equally to this work
*Correspondence: fkd2101@columbia.edu
DOI 10.1016/j.stem.2008.07.025

SUMMARY

Stem cells reside in specialized niches that regulate their self-renewal and differentiation. The vasculature is emerging as an important component of stem cell niches. Here, we show that the adult subventricular zone (SVZ) neural stem cell niche contains an extensive planar vascular plexus that has specialized properties. Dividing stem cells and their transit-amplifying progeny are tightly apposed to SVZ blood vessels both during homeostasis and regeneration. They frequently contact the vasculature at sites that lack astrocyte endfeet and pericyte coverage, a modification of the blood-brain barrier unique to the SVZ. Moreover, regeneration often occurs at these sites. Finally, we find that circulating small molecules in the blood enter the SVZ. Thus, the vasculature is a key component of the adult SVZ neural stem cell niche, with SVZ stem cells and transit-amplifying cells uniquely poised to receive spatial cues and regulatory signals from diverse elements of the vascular system.

INTRODUCTION

Adult neurogenesis occurs in two main regions of the mammalian brain: the subventricular zone (SVZ), which generates neurons destined for the olfactory bulb, and the subgranular zone (SGZ) of the hippocampal formation. In both regions, astrocytes, glial cells that have long been considered support cells in the brain, are neural stem cells (Doetsch, 2003). Within the adult SVZ, a subset of glial fibrillary acidic protein (GFAP)-expressing astrocytes (type B cells) are stem cells (Ahn and Joyner, 2005; Doetsch et al., 1999a; Garcia et al., 2004; Imura et al., 2003; Laywell et al., 2000; Sanai et al., 2004). Stem cell astrocytes divide to give rise to transit-amplifying type C cells, which, in turn, generate neuroblasts (type A cells) (Doetsch et al., 1999a). Neuroblasts migrate as chains through a network of pathways extending along the length of the SVZ and join the rostral migratory stream (RMS) that leads to the olfactory bulb, where they differentiate into inhibitory interneurons (Lledo et al., 2008). Identifying the unique features of adult neurogenic niches that regulate stem cell self-renewal and differentiation is key to understanding their in vivo stem cell regulation.

SVZ stem cells populate a complex niche adjacent to the lateral ventricles, whose components are just beginning to be uncovered. Ependymal cells that line the ventricles, long-distance axon projections that terminate in the SVZ, and an extensive basal lamina are all components of the SVZ stem cell niche (Riquelme et al., 2008).

The importance of the vasculature in stem cell and cancer stem cell niches is just emerging (Calabrese et al., 2007; Kiel et al., 2005; Louissaint et al., 2002; Nikolova et al., 2006; Palmer et al., 2000; Yoshida et al., 2007). Blood vessels are formed by endothelial cells and perivascular support cells, including pericytes and smooth muscle cells. Blood vessels themselves are ensheathed by a vascular basal lamina. Unlike in most organs, the blood-brain barrier (BBB) tightly regulates the transport of molecules between the blood and brain parenchyma (Zlokovic, 2008). Tight junctions between endothelial cells and astrocyte endfeet are integral components of the BBB (Abbott et al., 2006).

In the adult brain, a link has been suggested between angiogenesis and neurogenesis. In songbirds, testosterone-induced angiogenesis leads to recruitment of newly generated neurons into the high vocal center (Louissaint et al., 2002), and, in mammals, new neurons are born in close proximity to blood vessels at angiogenic foci in the hippocampus (Palmer et al., 2000). Indeed, diffusible signals from endothelial cells promote neural stem cell self-renewal in vitro (Shen et al., 2004). However, the role of the vasculature in vivo in the adult SVZ stem cell niche, the largest germinal area in the mammalian brain, remains unknown.

Here, we show that, in vivo, SVZ stem cells and their progeny are coupled to blood vessels in a specialized vascular niche. By using whole-mount preparations, we uncover a vascular plexus that spans the entire SVZ. Transit-amplifying C cells and stem cell astrocytes lie adjacent to blood vessels in this plexus, whereas most migrating neuroblasts are more distal to the vasculature. Intriguingly, stem cells and transit-amplifying C cells directly contact SVZ blood vessels at sites devoid of astrocyte endfeet as well as pericyte coverage both during homeostasis and regeneration. This specialized neurovascular interface is unique to the SVZ and

absent from nonneurogenic regions such as the cortex and striatum. Moreover, regeneration of the SVZ frequently occurs at these sites. We also find that the SVZ has direct access to signals derived from the blood. Thus, a distinctive vasculature in the adult SVZ niche is a key component of the specialized microenvironment supporting SVZ stem cells and their progeny.

RESULTS

Dividing Cells Lie Adjacent to Blood Vessels in the SVZ

To determine the structure of the vasculature in the SVZ and its relationship to dividing cells, we used confocal microscopy to analyze whole-mount preparations of the lateral wall of the lateral ventricle that allow the entire expanse of the SVZ to be visualized simultaneously (Doetsch and Alvarez-Buylla, 1996), unlike frontal sections, which need to be serially reconstructed. Whole mounts were immunostained with antibodies against CD31 (platelet/endothelial cell adhesion molecule) to label endothelial cells and Ki67 to label dividing cells. The SVZ contained an extensive planar vascular plexus that spans its entire length (Figure 1A). Large vessels entered the SVZ from the ventral and dorsal periphery of the lateral ventricles and extended long distances before branching into smaller vessels. In the dorsal-most aspect of the SVZ and in the RMS, blood vessels ran parallel to the direction of tangentially migrating neuroblasts (data not shown). This ordered planar structure differed from the vascular architecture in nonneurogenic brain regions, such as the cortex, which consisted of smaller vessels and capillaries that branched frequently (Figure 1B).

Blood vessels in the SVZ were ensheathed by a laminin-containing basal lamina (Figures S1A–S1C available online), which exhibited heterogeneity in the density of laminin staining along the vessels. Branched basal lamina structures, previously described as fractones (Mercier et al., 2002), extended from the SVZ vasculature and terminated in large bulb-shaped structures just under the ependymal layer (Figures S1A–S1C). Laminin-positive dots were also scattered over the entire wall of the ventricle. The origin of these dots is unclear, although some may correspond to the terminal bulbs of fractones (Figures S1A–S1C).

Strikingly, the vast majority of dividing cells lie adjacent to the SVZ planar vascular plexus (Figure 1C), including in caudal regions (Figures S1D and S1D′). Clusters of dividing cells that appeared to be some distance from the plexus were often associated with vessels perpendicular to the SVZ arising from the striatum (Figure S1E). Interestingly, not all blood vessels were associated with dividing cells, suggesting that SVZ blood vessels are heterogeneous and that specialized microdomains may be present within the vasculature. Blood vessels in the SVZ are largely capillaries, but dividing cells were also present adjacent to presumptive arteries and veins (Figure S1F). We did not observe proliferating endothelial cells, suggesting that there is little, if any, angiogenesis occurring in the vascular plexus under normal conditions. Furthermore, we did not observe endothelial tip cells, a hallmark of angiogenesis, in the adult SVZ, although they were abundant perinatally (Figure S2). Thus, unlike the SGZ (Palmer et al., 2000), the adult SVZ vasculature likely contains a relatively quiescent population of endothelial cells.

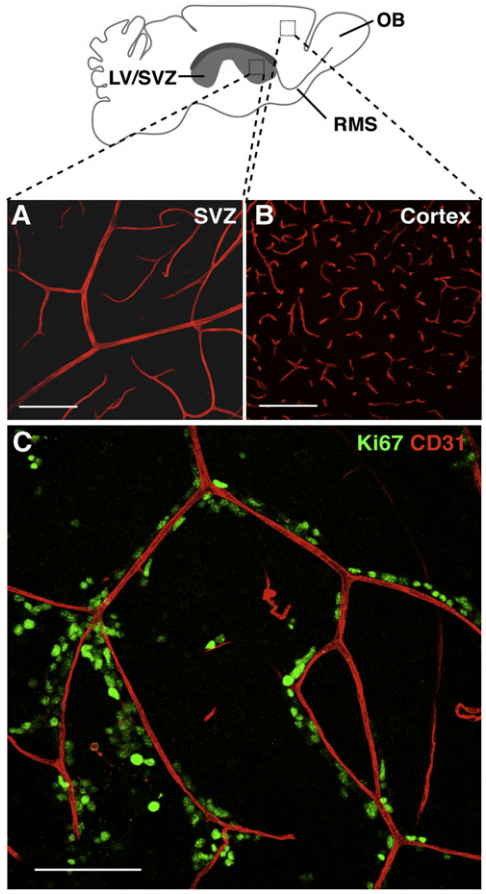

Figure 1. Dividing Cells Lie Adjacent to Blood Vessels in the SVZ

Schema of whole-mount dissection of the adult mouse brain depicting the entire lateral wall of the lateral ventricle (LV) and underlying SVZ (boxes indicate areas shown in [A] and [B]).

(A) Projection of confocal Z stack images of CD31 immunoreactive blood vessels in the SVZ, showing the planar architecture of the capillary plexus that runs parallel to the ventricular wall.

(B) Image of blood vessels in the cortex, where capillaries branch frequently in random directions and are more tortuous.

(C) Projection of Z stack images of the anterior SVZ in a whole-mount preparation double immunostained for the cell proliferation marker Ki67 (green) and endothelial marker CD31 (red). Note the close proximity of individual dividing cells and proliferating cell clusters to blood vessels. Not all blood vessels have dividing cells adjacent to them. RMS (rostral migratory stream), OB (olfactory bulb).

Scale bars, 100 μm.

Quantification of Association of SVZ Cell Types and Blood Vessels

To define the spatial relationship of cells at each stage in the SVZ stem cell lineage to the vascular plexus, we performed immunostaining for SVZ cell-type-specific markers and CD31 and measured the distance between the outer surface of SVZ blood vessels and the nuclei of individual cells. This analysis was performed on cells from all regions of the SVZ, including dorsal, ventral, rostral, and caudal aspects of the ventricle.

SVZ stem cells are a subset of glial fibrillary acidic protein (GFAP)-expressing astrocytes (Doetsch et al., 1999a). We

utilized a transgenic mouse line that expresses green fluorescent protein (GFP) under the control of *gfap* promoter elements (Zhuo et al., 1997) to visualize the cell body and processes of SVZ astrocytes. We first confirmed the specificity of GFP expression within the SVZ in GFAP::GFP mice (Figure S3). GFP was expressed in GFAP+ astrocytes (Figure S3A) and was absent in neurons (Figure S3B), ependymal cells (Figure S3C), and neuroblasts (Figure S3D). A small proportion of GFP+ astrocytes expressed the epidermal growth factor receptor (EGFR) (Figure S3F), as previously described (Doetsch et al., 2002). However, the majority of EGFR+ cells, which correspond to transit-amplifying C cells (Doetsch et al., 2002), were GFP-negative (Figure S3E). Thus, GFAP::GFP mice allow us to distinguish GFAP+ astrocytes within the SVZ.

Only a small subset of Ki67+ cells in the SVZ were GFP+ astrocytes (Figure 2A), and 51.2% (n = 22/43) of them directly contacted blood vessels. As previously described, dividing astrocytes had a simpler shape than the complex multipolar morphology characteristic of parenchymal astrocytes (Garcia et al., 2004). Sox2 is expressed in neural stem cells during development (Graham et al., 2003). We investigated whether it could also be used as a marker to identify stem cell astrocytes in the adult SVZ. However, Sox2 was highly expressed by all SVZ cell types (Figure S4) and could not be used as a unique marker of SVZ stem cells. Therefore, we used label retention as an alternative approach to identify putative stem cells. Label-retaining cells (LRCs) retain bromodeoxyuridine (BrdU) for extended periods due to their relatively long cell-cycle time (Cotsarelis et al., 1989; Potten and Morris, 1988; Spangrude et al., 1988). In contrast, rapidly dividing cells dilute the label, and differentiated progeny migrate away. GFAP::GFP mice were injected with BrdU and analyzed either immediately, to ensure that cell death was not being induced, or 6 weeks later to assess the distribution of GFP+ LRCs. At 1 hr after the final BrdU injection, 94% of cells were double labeled for both BrdU and Ki67, and only 1.6% were TUNEL+ (Figures S5A, S5B, and S5D), confirming that our labeling regime labeled dividing cells. At 6 weeks after labeling, 55.4% of label-retaining cells were adjacent to blood vessels, and 70% of GFP+ LR astrocytes were within 10 μm of blood vessels (Figures 2B, 2C, 3A, and 3B). GFP-expressing BrdU label-retaining astrocytes were significantly closer to blood vessels (11.2 μm) than nonlabel-retaining astrocytes (16.6 μm) ($p = 2.08 \times 10^{-05}$, Wilcoxin rank sum test; n = 1018 for nonlabel-retaining astrocytes, n = 55 for label-retaining astrocytes) (Figures 3A–3C). Thus, proliferating stem cell astrocytes were located in close apposition to blood vessels.

The vast majority of dividing cells adjacent to the vascular plexus were the highly proliferative transit-amplifying C cells (average distance 8.8 μm, n = 800), with 49.0% located within 5 um of blood vessels (Figures 2D, 2E, and 3A–3C). Transit-amplifying C cells express EGFR (Doetsch et al., 2002) and Mash1 (Parras et al., 2004). Most Ki67+ cells (85.3%, n = 151/177 cells) were EGFR+ (Figure 2E), and 81.2% (n = 329/405) of EGFR+ cells expressed Mash1 (Figure 2D). Moreover, transit-amplifying cells whose somas did not contact blood vessels frequently extended long processes toward the vasculature (data not shown).

In contrast to dividing SVZ astrocytes and transit-amplifying cells, most neuroblasts were less intimately associated with blood vessels (Figure 3D). We used doublecortin (Gleeson et al., 1999) as a marker for neuroblasts after confirming that its expression overlaps with PSA-NCAM and mCD24 (Calaora et al., 1996; Doetsch et al., 1997) (Figures S4E–S4G). While blood vessels ran parallel to the aggregates of chains of neuroblasts in the dorsal SVZ and RMS (data not shown), individual neuroblasts were largely not apposed to blood vessels (average distance 18.3 μm, n = 800 cells), and only 13.9% were within 5 μm of the vasculature (Figures 3A–3C). When chains of neuroblasts did intersect the vasculature, the blood vessels often dipped into the parenchyma away from the ventricle, allowing the chains of neuroblasts to pass through.

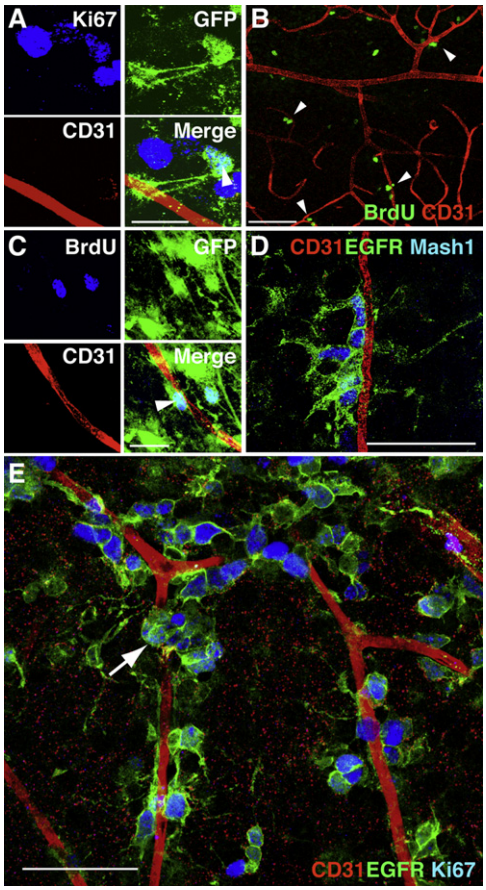

Figure 2. Stem Cell Astrocytes and Transit-Amplifying Cells Lie Adjacent to Blood Vessels in the SVZ

(A) A small fraction of dividing cells near blood vessels are astrocytes. Arrowhead points to Ki67+ (blue), GFP-expressing astrocyte (green) in GFAP::GFP mice. Scale bar, 20 μm.

(B) Many LRCs (green) are found adjacent to blood vessels (arrowheads). Scale bar, 50 μm.

(C) GFP+ LRCs (38% of all LRCs, arrowhead) are frequently found near blood vessels. Scale bar, 20 μm.

(D and E) The majority of dividing cells that lie adjacent to the SVZ vascular plexus are transit-amplifying C cells. (D) Most EGFR+ cells (green) express the C cell marker Mash1 (blue). (E) Z stack projection of whole-mount SVZ showing that the vast majority of Ki67 immunoreactive cells (blue) near blood vessels are EGFR+ (green). Often, these cells were found in clusters (arrow) near the vasculature. Scale bars, 50 μm.

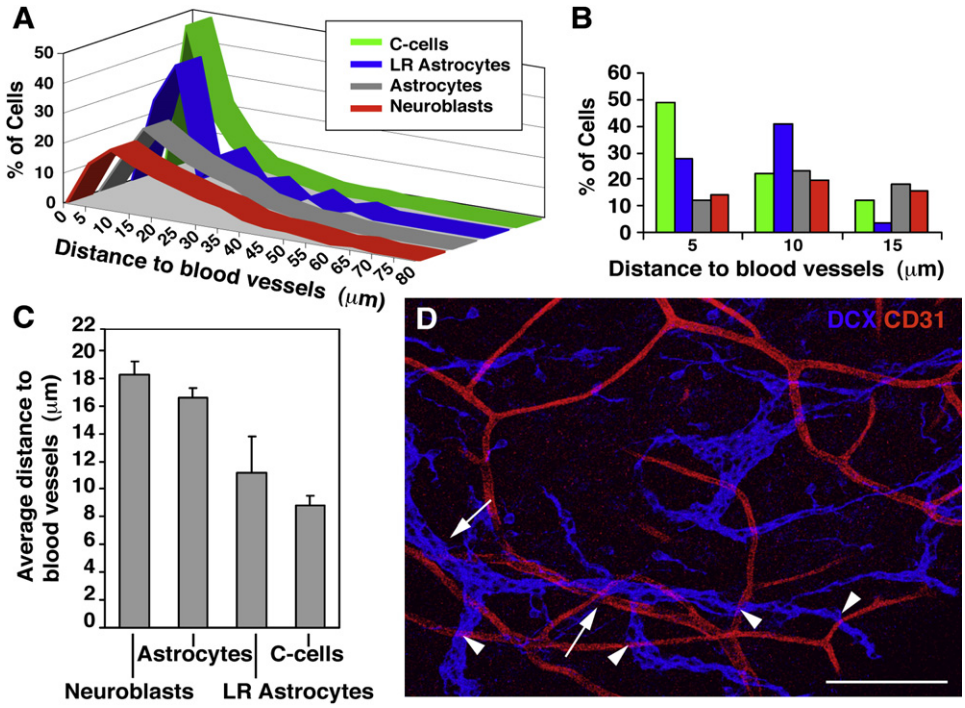

Figure 3. Quantification of the Distance of SVZ Cell Types to Blood Vessels

(A) Histogram depicting the distribution of distances to blood vessels for each SVZ cell type. (Green) Transit-amplifying C cells. (Blue) Label-retaining astrocytes. (Gray) Nonlabel-retaining astrocytes. (Red) Neuroblasts.

(B) Histogram depicting the first 15 μm of the distributions shown in (A) for each SVZ cell type. 49.0% of EGFR immunoreactive cells and 27.8% of label-retaining astrocytes are found within 5 μm of the vasculature, whereas only 13.9% of neuroblasts are. Pairwise comparisons of the distribution of distance measurements for all cell types revealed statistically significant differences ($p < 0.05$) between all cell types, except for neuroblasts and nonlabel-retaining astrocytes, which did not differ significantly ($p = 0.085$, Wilcoxin rank sum test).

(C) Histogram of the average distance (in μm) between individual cells and the nearest blood vessel for neuroblasts (18.3 μm), GFP+ nonlabel-retaining astrocytes (16.6 μm), GFP+ BrdU label-retaining astrocytes (11.2 μm), and C cells (8.8 μm). Error bars represent 2 × SEM.

(D) Z stack projection of whole-mount SVZ immunostained with antibodies against CD31 (red) and the neuroblast marker doublecortin (DCX, blue). In some instances, neuroblasts migrate short distances parallel to blood vessels (arrows). However, while they often cross over blood vessels (arrowheads), the majority of neuroblasts are less closely associated with the vasculature. Scale bar, 100 μm.

Vascular-Derived Signals Access the SVZ

The close association of SVZ stem cells and transit-amplifying cells with blood vessels suggests that they may receive important signals from the vasculature. To test whether blood-derived signals enter the SVZ, we perfused sodium fluorescein, a small molecular weight molecule (376 Da), into the blood using a protocol modified from Hawkins and Egleton (2006), and we examined whether sodium fluorescein was detected in the SVZ. In order to visualize the vasculature, we coinjected isolectins, which bind to the luminal walls of blood vessels as they flow through. Strikingly, we saw a high intensity of sodium fluorescein in the SVZ (Figure 4A) that was not present in other areas of the brain, such as the cortex (Figure 4B). The intensity was similar to that in the area postrema (Figure 4C), a brain region that is permeable to signals in the blood (Gross, 1992). Interestingly, the striatal, septal, and callosal walls of the lateral ventricle all exhibited a similar intense band of labeling, suggesting that all periventricular regions of the lateral ventricles have access to circulating factors. This labeling was most intense in sections at the level of the choroid plexus (Figure 4D). In addition to the broad band of diffuse staining throughout the SVZ, a higher intensity of fluorescence was observed near some isolectin-positive SVZ blood vessels (Figures 4E–4G). This suggests that small molecules from the blood may access the SVZ via two routes, directly from vessels in the SVZ vascular plexus and from vessels in the choroid plexus, which produces cerebrospinal fluid (CSF) that fills the ventricles.

Stem Cells and Transit-Amplifying Cells Contact Blood Vessels at a Specialized Neurovascular Interface

Although the SVZ is not classically thought to possess an altered BBB, the above tracer experiments suggest that the neurovascular interface of the SVZ may have unusual features. Therefore, we investigated the components of the BBB in SVZ blood vessels. The BBB is made up of tight junctions between endothelial cells. An integral component of the BBB is the endfeet of perivascular astrocytes, which envelop the abluminal surface of endothelial cells. In addition, pericytes are interposed between endothelial cells and astrocyte endfeet.

Tight junctions can be revealed by immunostaining for occludin, a component of tight junctions, and zonula occludens protein-1 (ZO-1), a protein that links tight junctions to the cytoskeleton (Abbott et al., 2006; Zlokovic, 2008). Tight junctions were present in SVZ blood vessels (Figures 4H and S6). However, at

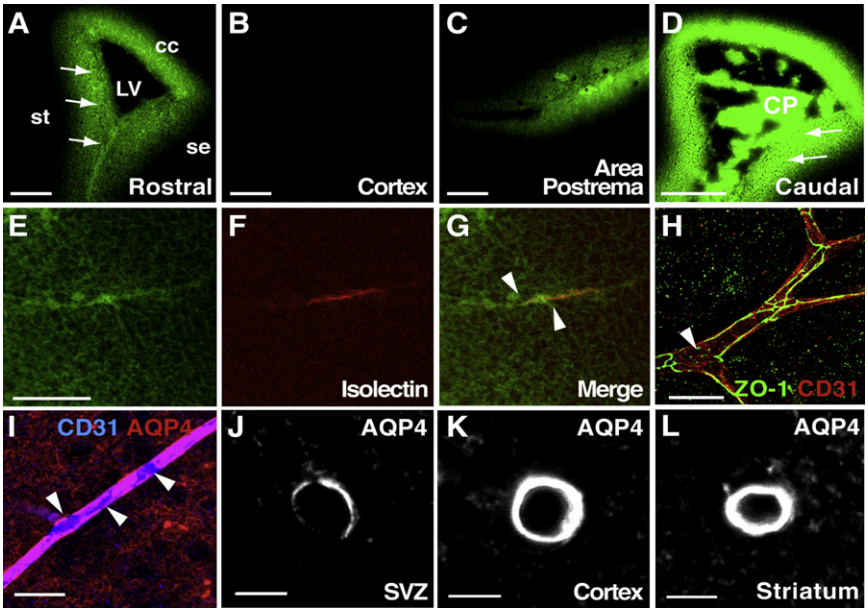

Figure 4. Vascular-Derived Signals Directly Access the SVZ

(A–G) Confocal images of frozen frontal sections of mice in which sodium fluorescein (green) and TRITC-labeled isolectins were perfused intracardially. Prior to perfusion, the descending aorta was cut to open the circulation to avoid acute hypertension during injection. All periventricular walls (st, striatum; se, septum; cc, corpus callosum), including the SVZ (arrows), were brightly labeled with sodium fluorescein (A) at a similar intensity to the area postrema (C). Note the absence of sodium fluorescein in the cortex (B). (D) Sodium fluorescein brightly labels the choroid plexus (CP) and adjacent periventricular walls at more caudal levels of the SVZ (arrows). Images in (A)–(D) were acquired at the same confocal settings. (E–G) While sodium fluorescein was diffusely distributed throughout the SVZ (E), some isolectin-positive vessels (F, red) had high concentrations of sodium fluorescein (green) directly surrounding them (arrowheads, E–G). Scale bars, (A–D) 100 μm; (E) 50 μm.

(H) Tight junctions are present in SVZ vasculature, although patches on some blood vessels appeared to lack tight junction staining (arrowhead).

(I) Immunostaining revealed areas (arrowheads) on CD31+ blood vessels (blue) in the SVZ lacking AQP4 staining (red). Scale bars, 20 μm.

(J–L) Confocal images acquired using identical confocal settings showing the intensity of AQP4 staining around average vessels from the SVZ (J), cortex (K), and striatum (L). AQP4 staining is much less intense around SVZ vessels as compared to vessels in nonneurogenic regions (cortex and striatum). Scale bars, 5 μm.

some sites, it appeared that SVZ vessels may lack tight junctions (Figures 4H and S6D), which would be consistent with the high density of sodium fluorescein adjacent to some vessels in the tracer experiments (Figures 4E–4G).

The endfeet of astrocytes can be visualized by immunostaining for Aquaporin-4 (AQP4), a water channel highly enriched in astrocyte endfeet at the BBB (Nico et al., 2001). Strikingly, small patches on blood vessels in the SVZ were devoid of AQP4 staining (Figures 4I and 4J), and EGFR-expressing cells often contacted the vasculature at these sites (Figures 5A, S7A, and S7B). The gaps in AQP4 staining were unique to the SVZ, as vessels from the cortex or adjacent striatum were completely ensheathed by astrocyte endfeet (Figures 4J–4L and S7C–S7E). Overall, AQP4 staining was much less pronounced in SVZ blood vessels as compared to the cortex and striatum. Ultrastructural analysis of the SVZ confirmed that transit-amplifying cells directly contact blood vessels at sites that lack astrocyte endfeet (Figures 5B–5D). Furthermore, pre-embedding immunostaining for AQP4 followed by electron microscopy (EM) confirmed that unlabeled glial endfeet were not present at sites at which transit-amplifying cells contact blood vessels (Figure 5B). Our EM analysis revealed that 38% of transit-amplifying cells contacted blood vessels directly at sites that lack astrocyte endfeet (n = 8/21). While large areas of direct contact were occasionally observed (Figure 5B), frequently, the sites of contact were small (Figures 5C, 5D, and S8), suggesting that they may be dynamic in nature.

We next examined the distribution of pericytes on SVZ blood vessels to determine whether sites that lacked AQP4 also exhibited withdrawal of pericytes. Pericytes can be visualized by immunostaining for NG2, a chondroitin sulfate proteoglycan. SVZ vessels were ensheathed by bright NG2+ cells (Figures 6A, 6B, and S9A–S9C). To confirm that these NG2+ perivascular cells were pericytes, and not progenitors that are present in the SVZ and throughout the brain (Aguirre et al., 2004; Nishiyama et al., 2002), we performed coimmunostaining for desmin, a marker of pericytes (Hellstrom et al., 1999) and EGFR. All perivascular NG2+ cells ensheathing the vessels expressed desmin (Figure 6C), and none expressed EGFR (0/64 cells) (Figure S9C). We observed three categories of EGFR+ cells contacting blood vessels: 40.4% contacted at sites that lacked both AQP4 and pericytes, 31% at sites that lacked pericytes but were AQP4+, and 28% at sites that had both AQP4 and pericytes (Figures 6D, 6E, S9D, and S9E). Thus, 71.4% of EGFR+ cells contacted blood vessels at sites that lacked pericyte coverage. The SVZ, therefore, contains a specialized neurovascular interface, which may support ongoing adult neurogenesis.

SVZ Regeneration Is Coupled to Blood Vessels

Our above findings reveal that dividing SVZ astrocytes and transit-amplifying cells are closely apposed to blood vessels during homeostasis. To assess whether the vasculature is relevant to SVZ stem cell function, we examined the relationship of stem cells to blood vessels during regeneration. After elimination of transit-amplifying cells and neuroblasts with the antimitotic drug cytosine-β-D-arabinofuranoside (Ara-C), stem cell astrocytes divide to rapidly regenerate the SVZ (Doetsch et al., 1999b). After Ara-C treatment, dying cells were distributed throughout the SVZ (Figures S5C and S5D), confirming that the drug was accessible to all dividing cells. At 12 hr after cessation of Ara-C treatment, when stem cell astrocytes begin to divide and regenerate the SVZ, 64.5% (n = 203 cells from three mice) of BrdU+ nuclei were superimposed directly on the vasculature

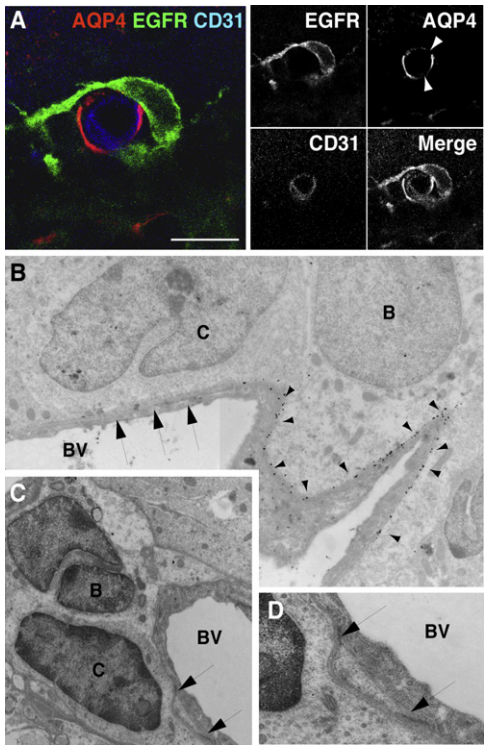

Figure 5. EGFR+ Transit-Amplifying C Cells Contact the Vasculature at Regions of Blood Vessels Lacking Astrocyte Endfeet

(A) Confocal images of SVZ blood vessels in cross-section showing transit-amplifying C cells (green) contacting the vasculature (blue) at AQP4-negative (red) patches (arrowheads) on blood vessels. Serial optical sections of cell in (A) are shown in Figure S7. Scale bar, 10 μm.

(B) Composite electron micrograph depicting contact between transit-amplifying C cell (labeled C) and blood vessel (BV) at a region of the vasculature that lacks AQP4 staining (arrows). Note the gold particles from AQP4 labeling (arrowheads) on the SVZ astrocyte (type B cell). Magnification, 15,800 ×.

(C and D) Electron micrographs showing an example of a transit-amplifying C cell (labeled C) directly contacting a blood vessel (BV). Image in (D) depicts high-power view of contact points shown in (C). A low-power view of this cell is shown in Figure S8. Magnification, (C) 15,800 ×; (D) 52,900 ×.

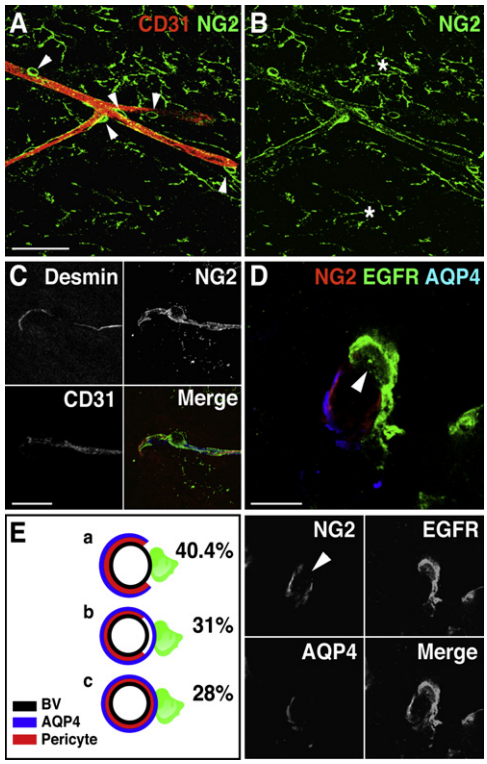

Figure 6. Transit-Amplifying C Cells Contact Blood Vessels at Sites Lacking Pericyte Coverage

(A and B) Distribution of NG2+ pericytes (green) along CD31+ blood vessels (red) in the SVZ. Note that NG2 is broadly expressed (asterisks), but perivascular NG2+ cells have a distinct morphology (arrowheads). Scale bar, (A) 50 μm.

(C) NG2+ perivascular cells in the SVZ express the intracellular pericyte marker Desmin. Scale bar, 20 μm.

(D) EGFR+ transit-amplifying C cells (green) contact the vasculature at sites (arrowhead) lacking pericyte coverage (NG2, red) and AQP4 staining (blue). Serial optical sections of cell in (D) are shown in Figure S9D. Scale bar, 10 μm.

(E) Schematic of proportion and types of contact with blood vessels (black circles) by EGFR+ cells (green) at (a) sites lacking both AQP4 (blue) and pericyte coverage (red), (b) sites with AQP4 coverage but no pericytes, and (c) sites with both AQP4 coverage and pericyte coverage.

(Figures 7A and 7D). None of these cells were TUNEL+ (Figures S5C and S5D). Newly appearing transit-amplifying cells were also directly coupled to the vasculature 2 days later (60.6%, n = 216) (Figures 7B–7D). These regenerating EGFR+ cells were frequently localized (43.4%, n = 23/53) at sites on the blood vessels that lacked AQP4 staining (Figure 7C). We did not detect any BrdU+ pericytes, BrdU+ endothelial cells, or upregulation of EGFR in pericytes at 7 days after pulsing with BrdU (data not shown). Thus, the SVZ vascular plexus acts as a scaffold for seeding regeneration of the SVZ niche, with regeneration frequently occurring at sites of the vasculature where cells exhibited direct contacts with blood vessels.

DISCUSSION

Our results show that the vasculature is an integral component of the SVZ stem cell niche, possessing unique properties that support stem cell proliferation and regeneration. Dividing cells—primarily stem cells and transit-amplifying cells—lie adjacent to the SVZ vascular plexus (Figure 7E) whose planar structure and composition is different from vessels in nonneurogenic brain regions. Intriguingly, patches of the SVZ vasculature lack coverage both by astrocyte endfeet and pericytes. We find that stem cells and transit-amplifying cells directly contact the vasculature at these sites. Furthermore, regeneration often occurs at these foci, highlighting their importance in supporting adult stem cell function. Strikingly, signals derived from the blood directly access the SVZ. As such, SVZ stem cells and transit-amplifying cells are uniquely poised to receive spatial cues and signals from the vasculature that regulate self-renewal and differentiation. These specialized features of the SVZ vasculature may underlie the high levels of neurogenesis in this region.

Interestingly, unlike the adult hippocampus, where active angiogenesis accompanies neurogenesis (Palmer et al., 2000), blood vessels in the adult SVZ seem to comprise a relatively stable vascular bed; we did not observe angiogenic sprouting of endothelial cells or endothelial cell division in the SVZ. Furthermore,

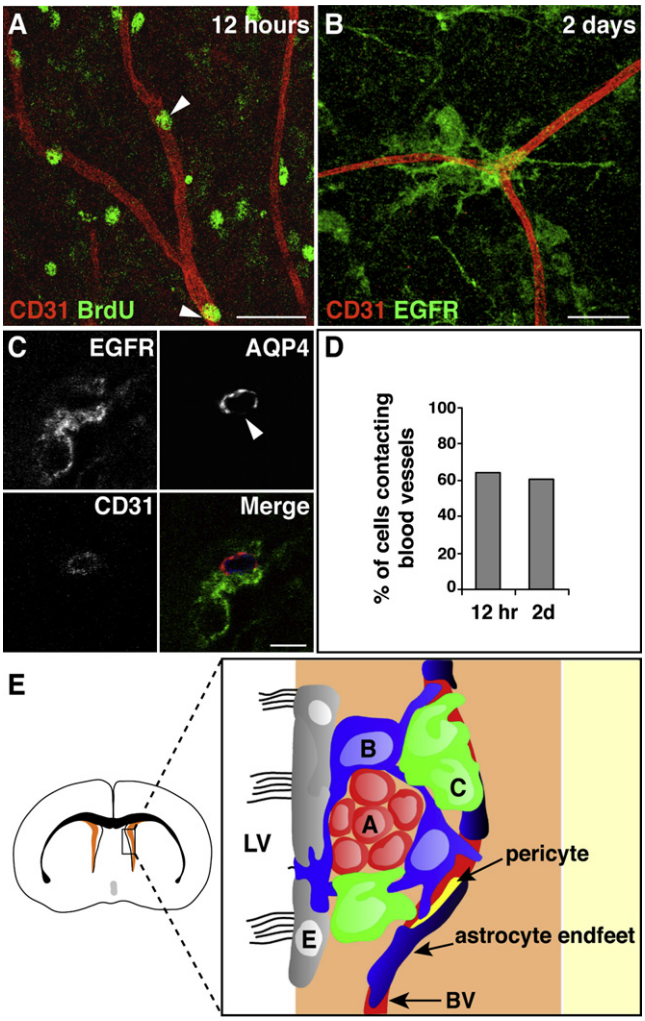

Figure 7. SVZ Stem Cells and Transit-Amplifying Cells Contact Blood Vessels during Regeneration

(A) At 12 hr after cessation of Ara-C treatment, BrdU+ cells in the SVZ (green, arrowheads) are immediately adjacent to the vasculature (red). Scale bar, 30 μm.

(B) After 2 days, EGFR+ C cells (green) contact blood vessels (red). Scale bar, 30 μm.

(C) Regeneration (EGFR+ cells, green) occurs at sites on blood vessels (blue) that lack AQP4 staining (red). Scale bar, 5 μm.

(D) Histogram showing percentage of cells contacting blood vessels at 12 hr and 2 days after cessation of Ara-C treatment.

(E) Model of the vascular SVZ stem cell niche. Schema of a coronal brain section, with SVZ in orange. Box is expanded to the right to show SVZ cells. Blood vessels (BV) are an integral component of the SVZ niche. Stem cell astrocytes (labeled B, blue) and transit-amplifying C cells (C, green) often contact the vasculature at regions on blood vessels lacking astrocyte endfeet (dark blue) and pericyte coverage (yellow), giving them direct access to vascular and blood-derived signals. Stem cell astrocytes also contact the lateral ventricle. Chains of neuroblasts (labeled A, red) are less closely associated with the vasculature. Ependymal cells (E, gray) line the lateral ventricles.

we did not observe gaps in astrocyte coverage in the SGZ (data not shown). As such, the two neurogenic niches may be fundamentally different. The unique architecture of the SVZ vascular niche may provide signaling cues that angiogenesis provides in the SGZ.

In the dorsal-most aspect of the SVZ and the RMS, we observed long blood vessels that paralleled the overall migration route of newly generated neurons. Blood vessels may thus facilitate the migration of neuroblasts as they traverse long distances in the brain. Indeed, once neuroblasts reach the olfactory bulb and escape the chains to migrate radially into the granule cell and periglomerular layers, they become tightly associated with blood vessels (Bovetti et al., 2007). However, at the individual cell level, tangentially migrating neuroblasts within the SVZ network of chains were not often closely coupled with the SVZ vascular plexus. It remains to be determined whether neuronal differentiation occurs in response to leaving the vascular bed or whether cells do so once they are committed to differentiation.

Some SVZ stem cells and transit-amplifying cells did not appear to be closely associated with the vasculature. These cells may, in fact, contact blood vessels deeper in the tissue or via long processes or may contact laminin-positive fractones that extend from vessels. Alternatively, these cells may be at different stages of activation or phases of the cell cycle. Relatively quiescent stem cells have been proposed to be maintained in hypoxic regions in other stem cell niches such as the bone marrow (Parmar et al., 2007). Once markers have been identified that allow the visualization of stem cell astrocytes, it will be possible to establish whether more quiescent SVZ stem cells also contact the vasculature or reside away from blood vessels.

Our findings reveal that the SVZ vascular niche is complex and encompasses diverse aspects of the vascular system. These include both diffusible signals and direct contact with endothelial and perivascular cells, the vascular basal lamina and associated fractones, as well as small molecules circulating in the blood. Endothelial cells are a source of diffusible signals, such as VEGF, FGF2, IGF1, PEDF, BDNF, and unidentified factors that affect neural precursors (Biro et al., 1994; Jin et al., 2002; Leventhal et al., 1999; Ramirez-Castillejo et al., 2006; Shen et al., 2004). In vivo, these factors may bind to the vascular basal lamina and to fractones that extend from the vasculature in the SVZ (Mercier et al., 2002), as has been shown for FGF2 (Kerever et al., 2007). As such, the rich vascular basal lamina and fractones present in the SVZ may be an important site of integration of niche signals arising not only from the vasculature, including pericytes, endothelial cells, and factors from the blood, but also from ependymal cells, mesenchymal cells, axon terminals, and the CSF. It will be important to further define the ECM molecules present in the SVZ and how they influence SVZ progenitors. Indeed, the laminin receptor α6β1 integrin is important for tethering SVZ progenitors to the vascular niche, and perturbation of this interaction affects adhesion and proliferation (Shen et al., 2008 [this issue of *Cell Stem Cell*]).

An unusual facet of the SVZ vascular niche is the direct contact that transit-amplifying cells and stem cells make with blood vessels at sites that lack astrocyte endfeet and pericyte coverage. These sites are unique to the SVZ and may be specialized microdomains that are important for stem cell regulation. It will be important to establish whether these gaps are stable specialized structures that provide enhanced access to different vascular components of the niche (direct contact with the basal lamina, endothelial cells, possible sites of diffusion of circulating factors) or whether they are dynamic, transitory structures

that arise as stem cell astrocytes retract perivascular processes when they become activated to generate transit-amplifying cells. We observed AQP4-negative gaps that lacked EGFR+ cells, suggesting that they may, at least in part, be stable structures. Identifying markers that distinguish stem cell astrocytes from niche astrocytes and defining whether stem cells themselves are AQP4+ will be helpful in determining whether stem cell astrocytes actively participate in forming the neurovascular interface.

Intriguingly, our tracer experiments reveal that vascular-derived small molecules have direct access to the SVZ, suggesting that the SVZ may have a modified BBB. Stem cells and transit-amplifying cells may, therefore, have greater access to molecules circulating in the bloodstream, such as growth factors, hormones, nutrients, and oxygen. It will be important to determine the size and identity of molecules that enter the SVZ from the blood. At present, we cannot distinguish whether small molecules arise from both the choroid plexus and SVZ vessels or only one source. Interestingly, SVZ astrocytes contact the CSF via a process that extends between ependymal cells (Doetsch et al., 1999b). These astrocytes also contact blood vessels (Shen et al., 2008). As such, stem cell astrocytes contacting the CSF may be poised to integrate signals from multiple niche compartments.

The specialized neurovascular interface of SVZ vessels and direct access of circulating factors we describe here also have important clinical implications for restorative neurogenesis and disease. In gliomas and multiple sclerosis (MS), one of the clinical features is withdrawal of astrocyte endfeet (Arismendi-Morillo and Castellano, 2005; Rafalowska et al., 1992), which may contribute to activation of endogenous progenitors in MS and invasive migration in gliomas. Indeed, glioma cells migrate and proliferate on cerebral blood vessels (Farin et al., 2006; Gilbertson and Rich, 2007). Furthermore, alterations in blood vessels that occur with aging (Burns et al., 1981; Hicks et al., 1983; Wilkinson et al., 1981) may underlie age-dependent decline of SVZ function (Luo et al., 2006; Molofsky et al., 2006; Tanaka et al., 2007). Finally, the SVZ may be more accessible to pharmacological agents, both toxic and therapeutic. This property of the SVZ stem cell niche may facilitate the stimulation of endogenous stem cells for brain repair.

Here, we identify the vasculature as an important component of the SVZ stem cell niche and uncover specialized features of the SVZ vasculature, including an altered BBB and access to blood-derived signals, that functionally distinguish blood vessels in the SVZ niche from nonneurogenic brain regions. Further defining how these unique elements of the niche interact will provide additional insight into the regulation of in vivo stem cell behavior.

EXPERIMENTAL PROCEDURES

Animal Use

Two- to 3-month-old CD1 (Charles River) GFAP::GFP mice (Jackson Laboratories) or TIE-2::GFP mice (Jackson Laboratories) were used in accordance with institutional guidelines.

Immunostaining

Whole mounts were immunostained as described (Doetsch and Alvarez-Buylla, 1996). See Supplemental Data for complete details. Briefly, whole mounts were blocked in 10% donkey serum (Jackson Immuno), incubated in primary antibodies overnight or 48 hr at 4°C, revealed with secondary antibodies (Jackson Immuno), and imaged using a Zeiss LSM510 confocal microscope. For SMA, AQP4, and NG2, immunostaining was also performed on 40 μm frontal sections. All immunostainings were done in triplicate.

BrdU Labeling

To identify LRCs, BrdU (Sigma) was injected intraperitoneally (28.5 μg/gm body weight) every 4 hr for a 12 hr period. Mice were either sacrificed immediately or 6 weeks later, and whole mounts were immunostained for BrdU (sheep 1:100; Fitzgerald Industries) as described (Doetsch et al., 1999b).

Quantification of Association of SVZ Cell Types and Blood Vessels

To quantify distances between cells and the vasculature, immunostaining for each SVZ cell type was performed, and high-magnification 30 μm Z stacks were taken from 15 randomly chosen fields in all regions of the SVZ of three different mice using a Zeiss LSM510 confocal microscope. Distances were measured from the estimated center of the nuclei of individual cells to the nearest blood vessel in each plane of the Z stack using Image-J software. Wilcoxin rank sum tests (assuming unequal variance) were used to determine statistical significance for comparisons of the distributions of distance measurements between the different cell types. To ensure that distances to blood vessels were not overestimated (due to the possibility that a blood vessel in a different Z plane could be closer to the cell of interest), all planes in the Z stack were evaluated for the presence of blood vessels in close proximity to the individual cells from any given plane.

Pre-Embedding Immunogold Labeling and EM

Brains were perfused with 0.5% glutaraldehyde/3% paraformaldehyde and postfixed overnight. Vibratome sections (50 μm) were cut and blocked in PBS/5% BSA/5% NGS for 30 min, rinsed in incubation buffer (1% BSA-C/PB), and incubated with antibodies against AQP4 (rabbit 1:250; Chemicon) for 24 hr at 4°C. Sections were revealed with secondary antibodies conjugated to ultrasmall (<1 nm) gold particles (1:100 Electron Microscopy Sciences) for 4 hr, washed, postfixed with 2.5% glutaraldehyde for 20 min, washed, postfixed with 1% osmium tetroxide for 1 hr, washed, and silver enhanced 20–30 min at room temperature. Immunostained sections were dehydrated and embedded in LX-112 resin (Ladd). Sixty nanometer sections were cut and collected on Formvar-coated single-slot grids, stained with uranyl acetate and lead citrate, and analyzed on a JEOL JEM-1200EX II microscope equipped with a Hamamatsu ORCA XR-60. The images were processed with AMT's CCD imaging system (version 5). Brains were processed for conventional EM as described (Doetsch et al., 1997).

Sodium Fluorescein Perfusion

We adapted the method from Hawkins and Egleton (2006). Briefly, mice were anesthesized and perfused intracardially with 9 ml of oxygenated Ringer solution containing 1 g/l sodium fluorescein (Sigma) and 0.02 g/l TRITC-labeled *Griffonia simplicifolia* Lectin (Sigma) over the course of 6 min. A large incision of the descending aorta was made immediately preceding the delivery of sodium fluorescein to open the vascular system to provide pressure relief and avoid hypertension. Brains were dissected and immediately frozen in tissue-freezing medium (Triangle Biomedical Sciences). Frozen sections (30 μM) were analyzed on a Zeiss LSM510 confocal microscope.

Ara-C Infusion

Ara-C mini-osmotic pumps were implanted as described (Doetsch et al., 1999b). Whole mounts were immunostained as described in the Supplemental Data 12 hr and 2 days after pump removal (n = 3 for each survival).

SUPPLEMENTAL DATA

The Supplemental Data include Supplemental Experimental Procedures and nine figures and can be found with this article online at http://www.cellstemcell.com/cgi/content/full/3/3/279/DC1/.

ACKNOWLEDGMENTS

We thank K. Brown for EM processing and N. Tjoe and A.J.P. Fink for technical assistance. We thank Jane Johnson for the Mash1 antibody and E. Crouch,

E. Drapeau, D. Medina, E. Pastrana, P. Riquelme, and S. Tavazoie for critical reading of the manuscript. M.T. is supported by MSTP fellowship T32 GM007367 from NIH, and L.V.d.V. is supported by a Belgian American Educational Foundation (BAEF) Fellowship for Graduate Study. V.S.-V. is a long-term HFSP fellow. L.C. is supported by T32 GM008224 from NIH, and F.D. is a Packard Foundation Fellow and Irma T. Hirschl Fellow. This work was partially supported by the Jerry and Emily Spiegel Laboratory for Cell Replacement Therapies and the Anne and Bernard Spitzer Fund for Cell Replacement Therapy.

Received: December 11, 2007
Revised: May 1, 2008
Accepted: July 29, 2008
Published: September 10, 2008

REFERENCES

Abbott, N.J., Ronnback, L., and Hansson, E. (2006). Astrocyte-endothelial interactions at the blood-brain barrier. Nat. Rev. Neurosci. *7*, 41–53.

Aguirre, A.A., Chittajallu, R., Belachew, S., and Gallo, V. (2004). NG2-expressing cells in the subventricular zone are type C-like cells and contribute to interneuron generation in the postnatal hippocampus. J. Cell Biol. *165*, 575–589.

Ahn, S., and Joyner, A.L. (2005). In vivo analysis of quiescent adult neural stem cells responding to Sonic hedgehog. Nature *437*, 894–897.

Arismendi-Morillo, G., and Castellano, A. (2005). Tumoral micro-blood vessels and vascular microenvironment in human astrocytic tumors. A transmission electron microscopy study. J. Neurooncol. *73*, 211–217.

Biro, S., Yu, Z.X., Fu, Y.M., Smale, G., Sasse, J., Sanchez, J., Ferrans, V.J., and Cassells, W. (1994). Expression and subcellular distribution of basic fibroblast growth factor are regulated during migration of endothelial cells. Circ. Res. *74*, 485–494.

Bovetti, S., Hsieh, Y.C., Bovolin, P., Perroteau, I., Kazunori, T., and Puche, A.C. (2007). Blood vessels form a scaffold for neuroblast migration in the adult olfactory bulb. J. Neurosci. *27*, 5976–5980.

Burns, E.M., Kruckeberg, T.W., and Gaetano, P.K. (1981). Changes with age in cerebral capillary morphology. Neurobiol. Aging *2*, 283–291.

Calabrese, C., Poppleton, H., Kocak, M., Hogg, T.L., Fuller, C., Hamner, B., Oh, E.Y., Gaber, M.W., Finklestein, D., Allen, M., et al. (2007). A perivascular niche for brain tumor stem cells. Cancer Cell *11*, 69–82.

Calaora, V., Chazal, G., Nielsen, P.J., Rougon, G., and Moreau, H. (1996). mCD24 expression in the developing mouse brain and in zones of secondary neurogenesis in the adult. Neuroscience *73*, 581–594.

Cotsarelis, G., Cheng, S.Z., Dong, G., Sun, T.T., and Lavker, R.M. (1989). Existence of slow-cycling limbal epithelial basal cells that can be preferentially stimulated to proliferate: implications on epithelial stem cells. Cell *57*, 201–209.

Doetsch, F. (2003). The glial identity of neural stem cells. Nat. Neurosci. *6*, 1127–1134.

Doetsch, F., and Alvarez-Buylla, A. (1996). Network of tangential pathways for neuronal migration in adult mammalian brain. Proc. Natl. Acad. Sci. USA *93*, 14895–14900.

Doetsch, F., Garcia-Verdugo, J.M., and Alvarez-Buylla, A. (1997). Cellular composition and three-dimensional organization of the subventricular germinal zone in the adult mammalian brain. J. Neurosci. *17*, 5046–5061.

Doetsch, F., Caille, I., Lim, D.A., Garcia-Verdugo, J.M., and Alvarez-Buylla, A. (1999a). Subventricular zone astrocytes are neural stem cells in the adult mammalian brain. Cell *97*, 703–716.

Doetsch, F., Garcia-Verdugo, J.M., and Alvarez-Buylla, A. (1999b). Regeneration of a germinal layer in the adult mammalian brain. Proc. Natl. Acad. Sci. USA *96*, 11619–11624.

Doetsch, F., Petreanu, L., Caille, I., Garcia-Verdugo, J.M., and Alvarez-Buylla, A. (2002). EGF converts transit-amplifying neurogenic precursors in the adult brain into multipotent stem cells. Neuron *36*, 1021–1034.

Farin, A., Suzuki, S.O., Weiker, M., Goldman, J.E., Bruce, J.N., and Canoll, P. (2006). Transplanted glioma cells migrate and proliferate on host brain vasculature: a dynamic analysis. Glia *53*, 799–808.

Garcia, A.D., Doan, N.B., Imura, T., Bush, T.G., and Sofroniew, M.V. (2004). GFAP-expressing progenitors are the principal source of constitutive neurogenesis in adult mouse forebrain. Nat. Neurosci. *7*, 1233–1241.

Gilbertson, R.J., and Rich, J.N. (2007). Making a tumour's bed: glioblastoma stem cells and the vascular niche. Nat. Rev. Cancer *7*, 733–736.

Gleeson, J.G., Lin, P.T., Flanagan, L.A., and Walsh, C.A. (1999). Doublecortin is a microtubule-associated protein and is expressed widely by migrating neurons. Neuron *23*, 257–271.

Graham, V., Khudyakov, J., Ellis, P., and Pevny, L. (2003). SOX2 functions to maintain neural progenitor identity. Neuron *39*, 749–765.

Gross, P.M. (1992). Circumventricular organ capillaries. Prog. Brain Res. *91*, 219–233.

Hawkins, B.T., and Egleton, R.D. (2006). Fluorescence imaging of blood-brain barrier disruption. J. Neurosci. Methods *151*, 262–267.

Hellstrom, M., Kalen, M., Lindahl, P., Abramsson, A., and Betsholtz, C. (1999). Role of PDGF-B and PDGFR-beta in recruitment of vascular smooth muscle cells and pericytes during embryonic blood vessel formation in the mouse. Development *126*, 3047–3055.

Hicks, P., Rolsten, C., Brizzee, D., and Samorajski, T. (1983). Age-related changes in rat brain capillaries. Neurobiol. Aging *4*, 69–75.

Imura, T., Kornblum, H.I., and Sofroniew, M.V. (2003). The predominant neural stem cell isolated from postnatal and adult forebrain but not early embryonic forebrain expresses GFAP. J. Neurosci. *23*, 2824–2832.

Jin, K., Zhu, Y., Sun, Y., Mao, X.O., Xie, L., and Greenberg, D.A. (2002). Vascular endothelial growth factor (VEGF) stimulates neurogenesis in vitro and in vivo. Proc. Natl. Acad. Sci. USA *99*, 11946–11950.

Kerever, A., Schnack, J., Vellinga, D., Ichikawa, N., Moon, C., Arikawa-Hirasawa, E., Efird, J.T., and Mercier, F. (2007). Novel extracellular matrix structures in the neural stem cell niche capture the neurogenic factor FGF-2 from the extracellular milieu. Stem Cells *25*, 2146–2157.

Kiel, M.J., Yilmaz, O.H., Iwashita, T., Yilmaz, O.H., Terhorst, C., and Morrison, S.J. (2005). SLAM family receptors distinguish hematopoietic stem and progenitor cells and reveal endothelial niches for stem cells. Cell *121*, 1109–1121.

Laywell, E.D., Rakic, P., Kukekov, V.G., Holland, E.C., and Steindler, D.A. (2000). Identification of a multipotent astrocytic stem cell in the immature and adult mouse brain. Proc. Natl. Acad. Sci. USA *97*, 13883–13888.

Leventhal, C., Rafii, S., Rafii, D., Shahar, A., and Goldman, S.A. (1999). Endothelial trophic support of neuronal production and recruitment from the adult mammalian subependyma. Mol. Cell. Neurosci. *13*, 450–464.

Lledo, P.M., Merkle, F.T., and Alvarez-Buylla, A. (2008). Origin and function of olfactory bulb interneuron diversity. Trends Neurosci. *31*, 392–400.

Louissaint, A., Jr., Rao, S., Leventhal, C., and Goldman, S.A. (2002). Coordinated interaction of neurogenesis and angiogenesis in the adult songbird brain. Neuron *34*, 945–960.

Luo, J., Daniels, S.B., Lennington, J.B., Notti, R.Q., and Conover, J.C. (2006). The aging neurogenic subventricular zone. Aging Cell *5*, 139–152.

Mercier, F., Kitasako, J.T., and Hatton, G.I. (2002). Anatomy of the brain neurogenic zones revisited: fractones and the fibroblast/macrophage network. J. Comp. Neurol. *451*, 170–188.

Molofsky, A.V., Slutsky, S.G., Joseph, N.M., He, S., Pardal, R., Krishnamurthy, J., Sharpless, N.E., and Morrison, S.J. (2006). Increasing p16INK4a expression decreases forebrain progenitors and neurogenesis during ageing. Nature *443*, 448–452.

Nico, B., Frigeri, A., Nicchia, G.P., Quondamatteo, F., Herken, R., Errede, M., Ribatti, D., Svelto, M., and Roncali, L. (2001). Role of aquaporin-4 water channel in the development and integrity of the blood-brain barrier. J. Cell Sci. *114*, 1297–1307.

Nikolova, G., Jabs, N., Konstantinova, I., Domogatskaya, A., Tryggvason, K., Sorokin, L., Fassler, R., Gu, G., Gerber, H.P., Ferrara, N., et al. (2006). The

vascular basement membrane: a niche for insulin gene expression and Beta cell proliferation. Dev. Cell *10*, 397–405.

Nishiyama, A., Watanabe, M., Yang, Z., and Bu, J. (2002). Identity, distribution, and development of polydendrocytes: NG2-expressing glial cells. J. Neurocytol. *31*, 437–455.

Palmer, T.D., Willhoite, A.R., and Gage, F.H. (2000). Vascular niche for adult hippocampal neurogenesis. J. Comp. Neurol. *425*, 479–494.

Parmar, K., Mauch, P., Vergilio, J.A., Sackstein, R., and Down, J.D. (2007). Distribution of hematopoietic stem cells in the bone marrow according to regional hypoxia. Proc. Natl. Acad. Sci. USA *104*, 5431–5436.

Parras, C.M., Galli, R., Britz, O., Soares, S., Galichet, C., Battiste, J., Johnson, J.E., Nakafuku, M., Vescovi, A., and Guillemot, F. (2004). Mash1 specifies neurons and oligodendrocytes in the postnatal brain. EMBO J. *23*, 4495–4505.

Potten, C.S., and Morris, R.J. (1988). Epithelial stem cells in vivo. J. Cell Sci. Suppl. *10*, 45–62.

Rafalowska, J., Krajewski, S., Dolinska, E., and Dziewulska, D. (1992). Does damage of perivascular astrocytes in multiple sclerosis plaques participate in blood-brain barrier permeability? Neuropatol. Pol. *30*, 73–80.

Ramirez-Castillejo, C., Sanchez-Sanchez, F., Andreu-Agullo, C., Ferron, S.R., Aroca-Aguilar, J.D., Sanchez, P., Mira, H., Escribano, J., and Farinas, I. (2006). Pigment epithelium-derived factor is a niche signal for neural stem cell renewal. Nat. Neurosci. *9*, 331–339.

Riquelme, P.A., Drapeau, E., and Doetsch, F. (2008). Brain micro-ecologies: neural stem cell niches in the adult mammalian brain. Philos. Trans. R Soc. Lond. B Biol. Sci. *363*, 123–137.

Sanai, N., Tramontin, A.D., Quinones-Hinojosa, A., Barbaro, N.M., Gupta, N., Kunwar, S., Lawton, M.T., McDermott, M.W., Parsa, A.T., Manuel-Garcia Verdugo, J., et al. (2004). Unique astrocyte ribbon in adult human brain contains neural stem cells but lacks chain migration. Nature *427*, 740–744.

Shen, Q., Goderie, S.K., Jin, L., Karanth, N., Sun, Y., Abramova, N., Vincent, P., Pumiglia, K., and Temple, S. (2004). Endothelial cells stimulate self-renewal and expand neurogenesis of neural stem cells. Science *304*, 1338–1340.

Shen, Q., Wang, Y., Kokovay, E., Lin, G., Chuang, S.-M., Goderie, S.K., Roysam, B., and Temple, S. (2008). Adult SVZ stem cells lie in a vascular niche: A quantitative analysis of niche cell-cell interactions. Cell Stem Cell *3*, this issue, 289–300.

Spangrude, G.J., Heimfeld, S., and Weissman, I.L. (1988). Purification and characterization of mouse hematopoietic stem cells. Science *241*, 58–62.

Tanaka, A., Watanabe, Y., Kato, H., and Araki, T. (2007). Immunohistochemical changes related to ageing in the mouse hippocampus and subventricular zone. Mech. Ageing Dev. *128*, 303–310.

Wilkinson, J.H., Hopewell, J.W., and Reinhold, H.S. (1981). A quantitative study of age-related changes in the vascular architecture of the rat cerebral cortex. Neuropathol. Appl. Neurobiol. *7*, 451–462.

Yoshida, S., Sukeno, M., and Nabeshima, Y. (2007). A vasculature-associated niche for undifferentiated spermatogonia in the mouse testis. Science *317*, 1722–1726.

Zhuo, L., Sun, B., Zhang, C.L., Fine, A., Chiu, S.Y., and Messing, A. (1997). Live astrocytes visualized by green fluorescent protein in transgenic mice. Dev. Biol. *187*, 36–42.

Zlokovic, B.V. (2008). The blood-brain barrier in health and chronic neurodegenerative disorders. Neuron *57*, 178–201.